Distributed flow sensing using optical hot -wire grid

Tong Chen, Qingqing Wang, Botao Zhang, Rongzhang Chen, and Kevin P. Chen*

Department of Electrical and Computer Engineering, University of Pittsburgh, 3700 O'Hara Street, Pittsburgh, Pennsylvania 15261, USA

kpchen@engr.pitt.edu

Abstract: An optical hot-wire flow sensing grid is presented using a single piece of self-heated optical fiber to perform distributed flow measurement. The flow-induced temperature loss profiles along the fiber are interrogated by the in-fiber Rayleigh backscattering, and spatially resolved in millimeter resolution using optical frequency domain reflectometry (OFDR). The flow rate, position, and flow direction are retrieved simultaneously. Both electrical and optical on-fiber heating were demonstrated to suit different flow sensing applications.

OCIS codes: (060.2370) Fiber optics sensors; (280.2490) Flow diagnostics.

References and links

1. H. H. Bruun, *Hot-Wire Anemometry: Principles and Signal Analysis* (Oxford University Press, 1995), Chap. 2.
2. Y-H. Wang, C-P. Chen, C-M. Chang, C-P. Lin, C-H. Lin, L-M. Fu, and C-Y. Lee, "MEMS-based flow sensors," Microfluid Nanofluid **6**(3), 333–346 (2009).
3. G. D. Byrne, S. W. James, and R. P. Tatam, "A Bragg grating based fibre optic reference beam laser Doppler anemometer," Meas. Sci. Technol. **12**(7), 909–913 (2001).
4. O. Frazão, P. Caldas, F. M. Araújo, L. A. Ferreira, and J. L. Santos, "Optical flowmeter using a modal interferometer based on a single nonadiabatic fiber taper," Opt. Lett. **32**(14), 1974–1976 (2007).
5. L. J. Cashdollar and K. P. Chen, "Fiber Bragg grating flow sensors powered by in-fiber light," IEEE Sens. J. **5**(6), 1327–1331 (2005).
6. C. Jewart, B. McMillen, S. K. Cho, and K. P. Chen, "X-probe flow sensor using self-powered active fiber Bragg gratings," Sen. Actuators A Phys. **127**(1), 63–68 (2006).
7. P. Caldas, P. A. S. Jorge, G. Rego, O. Frazão, J. L. Santos, L. A. Ferreira, and F. Araújo, "Fiber optic hot-wire flowmeter based on a metallic coated hybrid long period grating/fiber Bragg grating structure," Appl. Opt. **50**(17), 2738–2743 (2011).
8. S. Gao, A. P. Zhang, H. Y. Tam, L. H. Cho, and C. Lu, "All-optical fiber anemometer based on laser heated fiber Bragg gratings," Opt. Express **19**(11), 10124–10130 (2011).
9. W. Eickhoff and R. Ulrich, "Optical frequency domain reflectometry in single-mode fiber," Appl. Phys. Lett. **39**(9), 693–695 (1981).
10. U. Glombitza and E. Brinkmeyer, "Coherent frequency-domain reflectometry for characterization of single-mode integrated-optical waveguides," J. Lightwave Technol. **11**(8), 1377–1384 (1993).
11. B. Soller, D. Gifford, M. Wolfe, and M. Froggatt, "High resolution optical frequency domain reflectometry for characterization of components and assemblies," Opt. Express **13**(2), 666–674 (2005).
12. S. T. Kreger, D. K. Gifford, M. E. Froggatt, B. J. Soller, and M.S. Wolfe, "High resolution distributed strain or temperature measurements in single- and multimode fiber using swept-wavelengh interferometry," *Optical Fiber Sensors*, ThE42 (2006).
13. A. K. Sang, M. E. Froggatt, D. K. Grifford, S. T. Kreger, and B. D. Dickerson, "One centimeter spatial resolution temperature measurements in a nuclear reactor using Rayleigh scatter in optical fiber," IEEE Sens. J. **8**(7), 1375–1380 (2008).
14. M. Froggatt and J. Moore, "High-spatial-resolution distributed strain measurement in optical fiber with Rayleigh scatter," Appl. Opt. **37**(10), 1735–1740 (1998).
15. R. R. J. Maier, W. N. MacPherson, J. S. Barton, S. McCulloch, and B. J. S. Jones, "Distributed sensing using Rayleigh scatter in polarization-maintaining fibres for transverse load sensing," Meas. Sci. Technol. **21**(9), 094019 (2010).
16. T. Chen, Q. Wang, R. Chen, B. Zhang, C. Jewart, K. P. Chen, M. Maklad and P. R. Swinehart, "Distributed high temperature pressure sensing using air-hole microstructural fibers," Opt. Lett., **37** (to be published).
17. D. Coric, R. Chatton, H. G. Limberger, and R. P. Salathe, "High resolution liquid-level sensor based on fiber Bragg-gratings in attenuation fiber and optical low-coherence reflectometry," in *Optical Fiber Sensors*, 2006, Mexico.

#159670 - $15.00 USD Received 8 Dec 2011; revised 28 Feb 2012; accepted 28 Feb 2012; published 26 Mar 2012

18. D. Coric, R. Chatton, Y. Luchessa, H. G. Limberger, R. Salathe, and F. Caloz, "Light-controlled reconfigurable fiber Bragg grating written in attenation fiber," in *National Fiber Optic Engineers Conference*, 2007, paper JWA17.
19. T. Chen, D. Xu, M. Buric, M. Maklad, P. R. Swinhart, and K. P. Chen, "Self-heated all-fiber sensing system for cryogenic environments," Meas. Sci. Technol. **21**(9), 094036 (2010).
20. F. Ye, T. Chen, D. Xu, K. P. Chen, B. Qi, and L. Qian, "Cryogenic fluid level sensors multiplexed by frequency-shifted interferometry," Appl. Opt. **49**(26), 4898–4905 (2010).
21. T. Chen, M. Maklad, P. R. Swinhart, and K. P. Chen, "Self-heated optical fiber sensor array for cryogenic fluid level sensing," IEEE Sens. J, **11**, 1051 (2011).
22. M. Buric, T. Chen, M. Maklad, P. R. Swinehart, and K. P. Chen, "Multiplexable low-temperature fiber Bragg grating hydrogen sensors," IEEE Photon. Technol. Lett. **21**(21), 1594–1596 (2009).

1. Introduction

Measurements of the gas and liquid flow rates are essential to a wide range of applications, including weather and environmental monitoring, industrial process control, and gas/liquid pipeline operations. Among a variety of flow-meter designs, the classical hot-wire anemometry (HWA) is most widely adopted for industry applications due to its simple design and reliability. In a HWA, the flow rate is determined by interrogating the heat removal rate from hot wires/films by the blowing gas/liquid [1]. Thanks to the development of micro electro mechanical systems (MEMS) technology in the last 20 years, miniature HWAs can be fabricated on chip to perform single-point flow measurements with high sensitivity, fast response time, and minimum power consumption [2]. However, in many industrial setting, flow sensing applications such as detecting gas pipe leaks, or monitoring gas flows in combustion engines, the scale of the flow field and harsh working environments post significant challenges to the existing HWA flow sensors. For example, to fully characterize the three dimensional vector flow field, large amount of hot wire sensors are needed to measure both magnitudes and directions of the flow field. This incurs cost and wiring difficulties especially at cryogenic or high temperatures or in corrosive and radioactive environments.

Fiber optic sensors are well-known for both working under harsh environment and the capability of sensor multiplexing, thus become a good candidate for harsh environment flow measurements. Many fiber flow sensors have been reported using different measurement schemes, including Doppler anemometer [3], bending flow sensor [4], and fiber HWAs [5–8]. For fiber based hot-wire flow sensors, a variety of delicate on-fiber heating designs have been proposed, including using single-mode-multimode tap [5,6], long period grating (LPG) [7], and high attenuation fibers [8]. Local gas flow rate is associated with the flow-induced temperature drop, which is measured by the Fiber Bragg gratings (FBGs) inscribed in the heat release area of the fiber. The sensitivity, response time and dynamic range of HWA can be controlled by changing the on-fiber heating profile. Efforts have also been made to obtain multi-dimensional flow information. An *X*-probe configuration using two multiplexed fiber HWAs was also reported for simultaneous measurement of flow magnitude and direction [6]. By multiplexing many heated FBG sensors in one fiber, flow rate at multiple locations can be interrogated for many harsh environment applications. However, the spatial resolution of the flow field measurement is limited by FBG sensor multiplexing density and the associated manufacturing cost.

Optical frequency domain reflectometry (OFDR) technology has been developed in the last thirty years for the purpose of ultra-fine resolution distributed sensing. Compared with optical time domain reflectometry (OTDR), the resolution of which is limited to ~0.1-1-m range by the temporal resolution of the system, OFDR provides superior spatial resolution down to ~10-μm with frequency-space conversion technique [9,10]. The OFDR scheme utilizes a sweep-wavelength interferometry to spatially resolve the measurement location, this requires an elastic process such as Rayleigh scattering to ensure the optical coherence. Recently, integration of in-fiber Rayleigh backscattering measurements with OFDR technology were reported by M. Froggatt, *et al.*, and has been employed for a variety of applications including fiber diagnosis [11] and distributed sensing of multiple parameters such as temperature [12,13], strain [12,14,15], and pressure [16].

#159670 - $15.00 USD Received 8 Dec 2011; revised 28 Feb 2012; accepted 28 Feb 2012; published 26 Mar 2012

In this paper, we proposed a multi-layer hot-wire grid anemometer using a single piece of self-heated fiber without the need of FBG sensors. By spatially resolving the in-fiber Rayleigh backscattering signal in the heated fiber using the OFDR technique, temperature profiles along all sections of the heated fiber grid are measured and synthesized to generate a comprehensive picture of the gas flow vector field, including the rate, position and direction of the flow field with millimeter spatial resolution. By using a single piece of fiber as the sensing device, the proposed sensor design completely eliminates the needs and associated costs for large number of FBG point sensors, thus provides a low-cost, reliable and powerful tool for comprehensive flow sensing applications for all environments.

2. Sensing principle and experimental setup

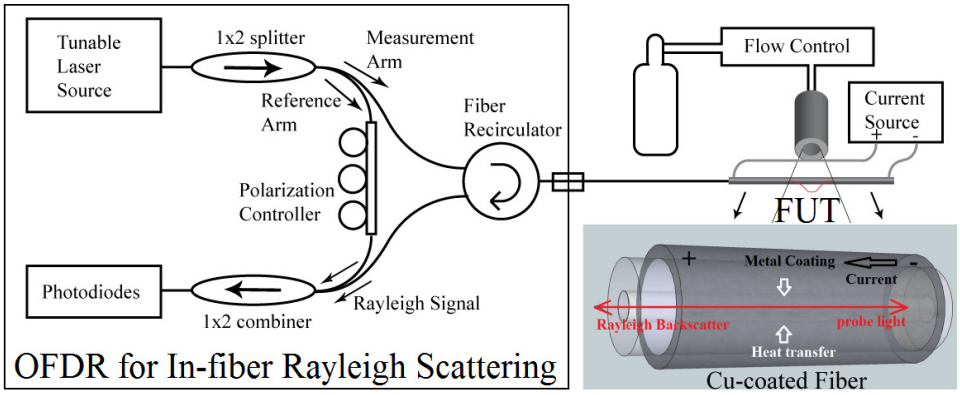

Fig. 1. The schematic of in-fiber Rayleigh scattering measurement for flow sensing using OFDR and electrically heated fiber.

Rayleigh scattering in optical fiber is caused by the statistical fluctuation in material density of the doped silica core. It is directly related to distributed fiber parameters such as transmission gain and loss, locally induced temperature, strain, and birefringence perturbations. The principle of flow sensing using the spatially resolved Rayleigh scattering in self-heated fiber can be explained using the OFDR diagram as shown in Fig. 1. Probe light from a CW laser is linearly swept in frequency as $\omega(t) = \omega_0 + \gamma t$, in which γ is the wavelength tuning rate and t is the time. The sweeping light is coupled into a fiber interferometer, in which the measurement arm is connected to the fiber under test (FUT) using a fiber circulator, and the reference arm is connected to a polarization controller. The excited Rayleigh scattering in the FUT is reflected back to the OFDR and recombined with the probe light in the reference arm with different frequency. This frequency difference is due to the path difference in the interferometer, and is associated with the location where Rayleigh scattering is excited. Beating signals between the reference light E_{ref} and Rayleigh backscattered measurement signal E_{meas} are received on the photodiodes as [14],

$$I_{beat}(\omega) = 2E_{ref}(t) \cdot E_{meas}(t-\tau) \cdot \rho(\omega)\cos[\omega\tau - \phi] \quad (1)$$

in which ρ and ϕ are the Rayleigh gain and phase shift, and the time delay τ between measurement and reference arms is directly related to the fiber location as $\tau = nx/c$, with x being the length difference between two arms, c being the speed of light and n being the effective refractive index of the FUT. The spatial-resolved Rayleigh response can be decoded using a fast Fourier transform (FFT) of $I_{beat}(\omega)$ upon the sweeping wavelength ω,

$$I(\tau) = I(n_f x) = FFT[I_{beat}(\omega)] \quad (2)$$

The maximum interrogating length and the spatial resolution are determined by [14],

#159670 - $15.00 USD Received 8 Dec 2011; revised 28 Feb 2012; accepted 28 Feb 2012; published 26 Mar 2012

$$L_{\max} = c\tau_{sampling}/4n, \Delta L = \pi c/n\Delta\omega_{sweep} \quad (3)$$

where $\tau_{sampling}$ is the sampling rate of the photodiode, and $\Delta\omega_{sweep}$ is the sweeping range of angular frequency. By cross-correlating with a pre-measured reference, Rayleigh spectral shifts induced by external perturbations such as temperature along the FUT can also be spatially interrogated as [12],

$$I_{measure}(\omega) \otimes I^{*}_{ref}(\omega) = FFT\left[I_{measure}(\tau) \cdot I^{*}_{ref}(\tau)\right] \quad (4)$$

$$K_T \Delta T = \Delta\lambda/\lambda = -\Delta\nu/\nu \quad (5)$$

where K_T is the effective temperature response coefficient that combines the elasto-optic and thermal expansion coefficient. To obtain a higher temperature resolution, a larger cross-correlation window is needed, at the cost of spatial resolution. The space-temperature resolution product can be expressed as [12],

$$\Delta L_{cc}(\Delta\lambda/\lambda) = \Delta L(K_T \Delta T) = \lambda/4n \quad (6)$$

To apply the OFDR technique for flow sensing, a commercial OFDR unit (Luna Technologies, OBR 4600) is butt coupled to a piece of metal-coated fiber as the FUT. With 90-nm wavelength tuning range at 1560-nm central wavelength and 2MB/s sampling rate, the maximum interrogation fiber length and spatial resolution are 70-m and 10-μm respectively according to (3). When a 1-cm long cross-correlation window is applied for the measurement and reference Rayleigh spectra, local temperature can be measured with 0.1°C accuracy with conventional optical fibers. The FUT was a piece of single-mode telecom optical fiber with 9-μm diameter Ge-doped core and 125-μm cladding, coated with 20-μm thick of Copper alloy (Oxford Electronics, SM1300-125CB). Electrical current is applied to the metal surface of the fiber to generate resistive heat along the fiber, which can be spatially interrogated using the in-fiber Rayleigh scattering unit. When gas flow is blowing on a section of the FUT, the OFDR Rayleigh measurement is taken and compared with the first measurement without the gas flow. The magnitude and position of flow-induced heat loss is determined by the temperature drop along the heated fiber.

#159670 - $15.00 USD Received 8 Dec 2011; revised 28 Feb 2012; accepted 28 Feb 2012; published 26 Mar 2012

3. Flow sensing results with electrical heated fiber

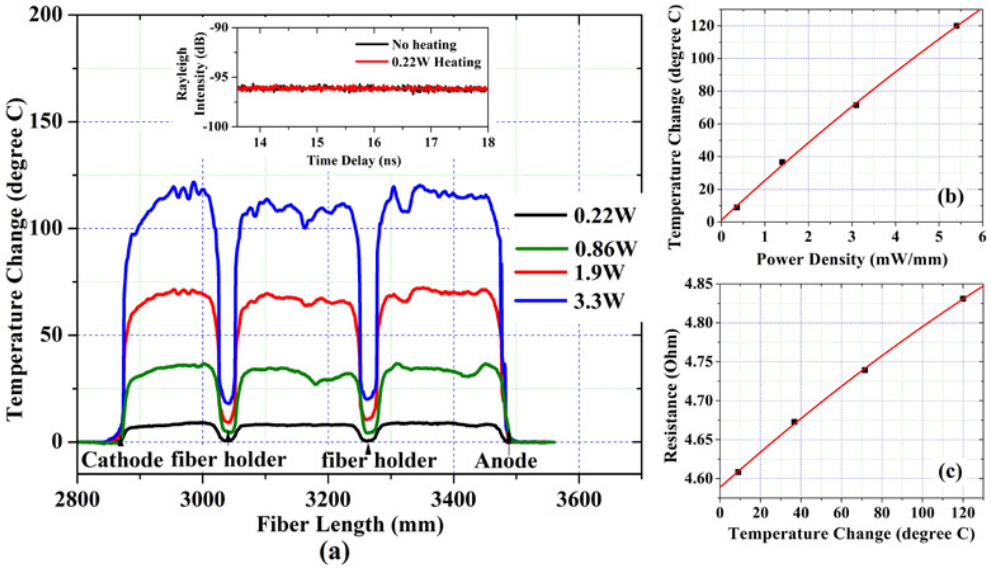

Fig. 2. (a) The heating profiles along the FUT for different input power, derived from the cross-correlation between unheated and heated Rayleigh spectra; Inset: unheated and 0.22W heated Rayleigh spectra (b) The heating efficiency vs. input power density, values obtained at fiber length of 3470mm in 2a; (c) The temperature dependence of resistance.

Figure 2a shows the temperature profile of a piece of electrically heated fiber from OFDR Rayleigh measurements without the gas flow with various input electrical heating power. Effective temperature response coefficient of –0.67GHz/°C [13] is used for the 20-μm thick copper-alloy coated fiber to correlate the measured Rayleigh spectral shifts with distributed temperature changes. The non-uniform temperature profile can be attributed to the coating imperfection. When the input power increases, the imperfect coating causes similar temperature profile along the fiber. The tunability of electrical on-fiber heating is further demonstrated with the dependence plot of on-fiber temperature rise vs. input power density in Fig. 2b. The temperature dependence of fiber resistance is shown in Fig. 2c, which explains the slight nonlinearity revealed by Fig. 2b.

To simultaneously determine the magnitude and direction of the gas flow, a single heated fiber is folded into two parallel hot optical wires spaced 10-mm apart as shown in insets of Fig. 3. In this configuration, gas nozzles were arranged in the same plane of the two hot wires. This allows the determination of flow direction in the same plane as the hot optical wires. The optical fiber is electrically heated to ~110°C above the ambient temperature. Multiple flow parameters are interrogated using this configuration, which include flow rate, transverse position and tilting angle of the flow vector, and multiple flows.

#159670 - $15.00 USD Received 8 Dec 2011; revised 28 Feb 2012; accepted 28 Feb 2012; published 26 Mar 2012

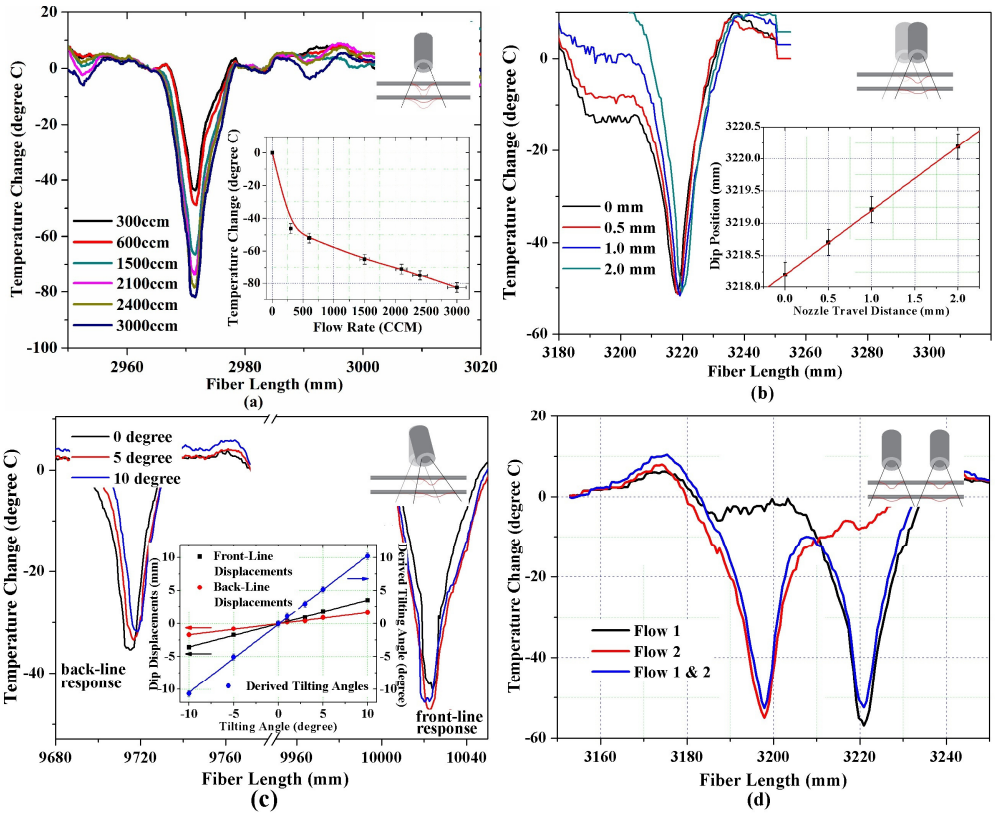

Fig. 3. (Color Online) The heat loss profiles and sensor responses of (a) flow rate measurement; (b) flow transverse position measurement; (c) flow direction measurement (d) two gas flows measured simultaneously.

Figure 3a shows the thermal response of the front-line hot optical wire to 300-3000-ccm (cubic centimeter per minute) gas flows blown from a ¼-inch nozzle 5-mm away. Flow rate of nitrogen gas is regulated with a calibrated mass flow controller, with 1000-ccm corresponding to 0.527m/s at the nozzle. To simplify the model, we assume laminar flow in our discussion. According to the HWA theory [1], the heat loss H_{loss} can be related to the flow rate v as,

$$H_{loss} = \Delta T\left(A + B\sqrt{v}\right) \tag{7}$$

where ΔT is the temperature rise on the HWA, A and B are empirical coefficients. For flow rates increased from 300 to 3000-ccm (0.158-1.58-m/s at the nozzle), the inset of Fig. 2a shows the decreasing of dip temperatures from −46°C to −80°C. With electrical heating power density of 5.4-mW/mm, A = −0.026-mW/mm/°C and B = 0.011-mW/mm/°C/(m/s)$^{1/2}$ were obtained from curve fitting. The flow sensitivity at 0.263-m/s (500-ccm) is 0.014-m/s/°C.

In additional to the conventional flow rate measurement, transverse position of the flow can also be monitored with the thermal profile of the hot optical wires, as shown in Fig. 3b. The inset shows the 1:1 linear dependences of the Gaussian-fitted dip position on the hot optical wire to the reading on translation stage of the gas nozzle. Sub-millimeter transverse movements of the gas-blowing nozzle can be readily differentiated with ± 0.2-mm resolution.

Furthermore, tilting of the gas-flow directions can be discriminated from transverse movements using the two parallel hot optical wires configuration. As is shown in Fig. 3c, with a tilting flow, the frontline heat loss profile is moving to the left positions and backline profile

#159670 - $15.00 USD Received 8 Dec 2011; revised 28 Feb 2012; accepted 28 Feb 2012; published 26 Mar 2012

to the right due to the fiber folding. Tilting angle θ_x can be related to the deviation difference using basic trigonometric calculation as,

$$\theta_x = \arctan\left[\left(\Delta x_{back} - \Delta x_{front}\right)/d\right] \tag{8}$$

where Δx_{front} and Δx_{back} are the deviation of front and backline dip position respectively, and d is the spacing between front and backline, set as 10-mm. The inset of Fig. 3c shows the measured Δx_{front} and Δx_{back}, and the derived θ_x for actual tilting angles from −10° to + 10°. Good sensing accuracy with less than 5% error is obtained, which could be further enhanced with larger spacing d. Figure 3c also shows that the temperature change and flow sensitivity decreases with larger nozzle-fiber distance. The sensitivity at the backline fiber is approximately 25% smaller than that of the frontline fiber.

Finally, multiple gas flows can be detected at the same time. We alternatively turned on and off two independent gas flows 23-mm apart from each other, and the measured thermal profiles clearly verified our operations, as is shown in Fig. 3d.

To measure flow directions in two-dimension (2D) simultaneously, a 15-section two-layer 2D grid is formed using a long piece of heated fiber in 4 × 4 + 3 × 4 configuration as shown in Fig. 4a and 4b. They are labeled as X1/Y1 front grid and X2/Y2 back grid separated by 10 mm. The X1 horizontal fiber lines are separated from the Y1 vertical fiber lines by 5-mm. So is the case for the X2 and Y2 fiber lines.The backlines are also interleaved between frontlines, as is shown in the insets of Fig. 4d and 4e. When a gas flow is applied to the grid, all 15 possible heat loss dips are monitored with a single scan, as is shown in Fig. 4c. The 2-D hot optical grid allows the determination of the 2D location of the gas nozzle (x, y) and the blowing directions (θ_x, θ_y) simultaneously. Figure 4d-e presents an example of the calibration process. Figure 4d shows the heat loss amplitudes with constant gas flow of 1200-ccm, when the flow is travelling in Y-axis direction from −5-mm to + 10-mm, passing two frontlines and two backlines of optical hot wires along the x axis. Figure 4e shows the same heat loss amplitude correction measurement for flow tilting angle from −10°C to 10°C in Y-axis. A flow attenuation matrix for $v_{measured}$ can be constructed using this calibration process for both X and Y axes. Using the calibration matrix, we took two measurements at actual 2-D positions of the nozzle and flow rates of (x = 3.0 mm, y = 3.0 mm, 1800-ccm) and (x = −2.0 mm, y = −4.0 mm, 1200-ccm) at (θ_x = 0°, θ_y = 0°) and retrieved the measured position and flow rate values, as are shown in Fig. 4f. Another two measurements were taken for actual 2-D tilting angles and flow rates of (θ_x = −3.0°, θ_y = −3.0°, 1800-ccm) and (θ_x = 5.0°, θ_y = 5.0°, 1200-ccm) at (x = 0 mm, y = 0 mm) and the measured values are also retrieved from the calibration, as shown in Fig. 4f. For both cases, the measured and actual values showed good agreements with maximum offsets <4% in the 3-D measurement spaces.

#159670 - $15.00 USD Received 8 Dec 2011; revised 28 Feb 2012; accepted 28 Feb 2012; published 26 Mar 2012

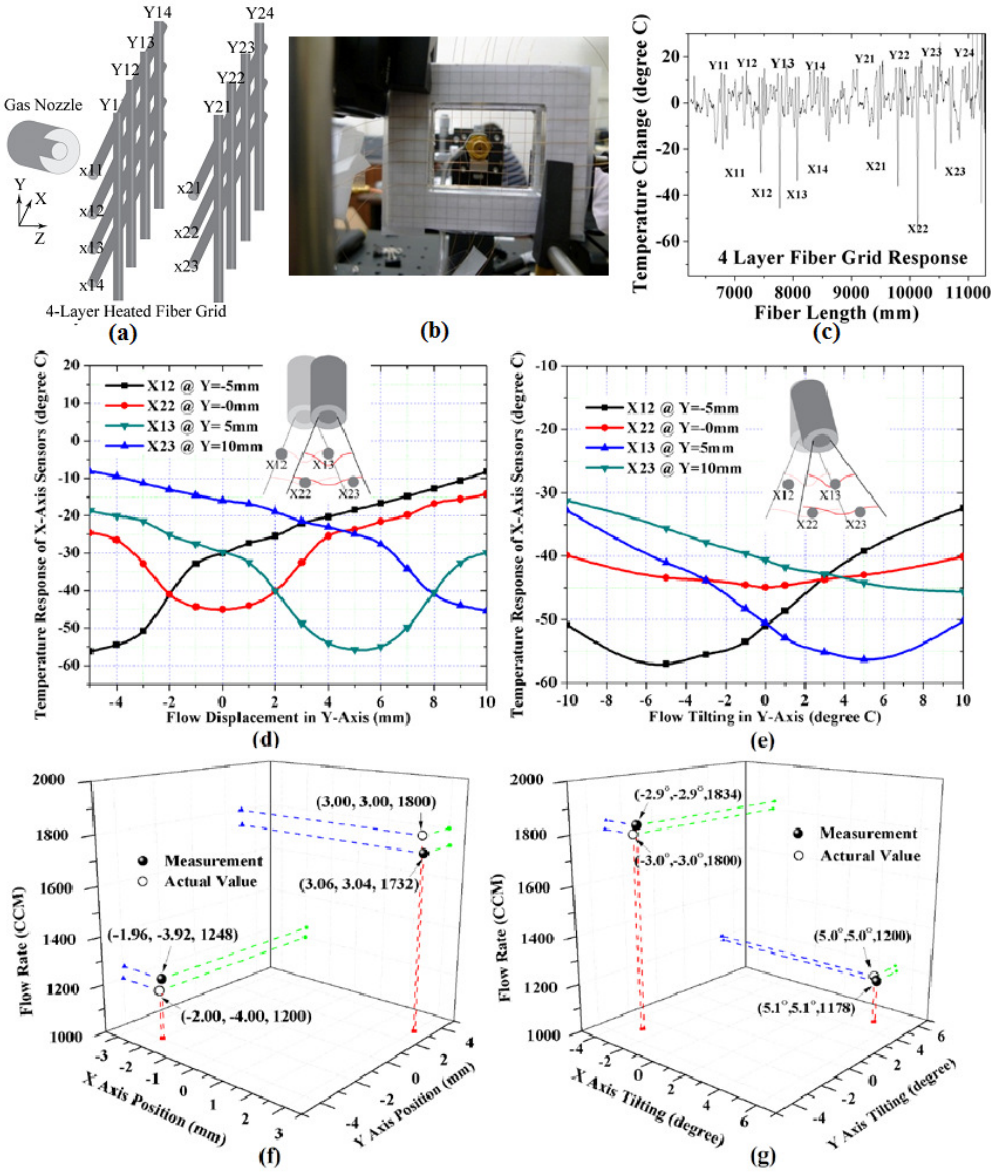

Fig. 4. (a) The schematic and (b) the picture and (c) the flow response of a 4-layer fiber hot-wire grid with 15 HWA sections; (d, e) The calibration curve of flow rate with longitudinal movements and angle tilting; (f, g) The comparison between measured and actual values of flow rate, positions and angles.

4. Flow sensing with optically heated fiber

The electrical on-fiber heating is uniform, low-cost, and energy efficient. But several disadvantages limited its employments in advanced sensing applications. The electrical heating current is prone to electromagnetic interferences (EMI), and environmental conductivities. It also presents spark hazard with flammable gas. The metal coating is vulnerable to corrosive chemicals, and the resistivity of metal decreases dramatically at low temperature. To overcome these problems, we proposed replacing electrical heating with optical on-fiber heating using single-mode high attenuation fiber (HAF). The idea of heating a piece of single-mode fiber internally via the absorption of optical power in HAF was first

#159670 - $15.00 USD Received 8 Dec 2011; revised 28 Feb 2012; accepted 28 Feb 2012; published 26 Mar 2012

proposed by Coric et al. [17,18], and was employed for a variety of fiber sensing applications including room and cryogenic temperature liquid level sensors [17,19–21], cryogenic hydrogen gas sensors [19,22], and gas flow sensors [8]. As illustrated in Fig. 5a, >1W amplified heating light at 1550-nm is combined with the tunable light at 1560-1610nm from OFDR unit using a bidirectional fiber coupler and injected into HAF under test. Optical power is attenuated in the HAF core and transformed into heat power and transferred to the fiber surface. Figure 5c shows the temperature profile and heating efficiency of an optically heated 0.05-dB/mm loss HAF. Contrary to the uniform electrical heating, exponential decays of temperature changes along the HAF were observed due to optical attenuation. With 600-mW input optical power at 1550-nm, the HAF can be heated up by 50-140°C in 100-cm fiber length. The smooth and stable temperature profiles due to internal fiber heating provide an excellent test-bed for gas flow sensing. The sensor responses of 0-500-ccm (0-0.263-m/s) gas flows from a ¼-inch nozzle 5-mm away are shown in Fig. 5d. The dip temperatures decreased from −10°C to −31°C for flow rate from 50 to 500-ccm (0.0263-0.263-m/s). With optical heating power density of 6.8-mW/mm at fiber length position of 16-mm, A = 0.067-mW/mm/°C and B = 0.19-mW/mm/°C/(m/s)$^{1/2}$ were obtained from curve fitting. The flow sensitivity at 0.263-m/s (500-ccm) is 0.020-m/s/°C. This value is slightly larger than the sensitivity obtained with electrical heating scheme.

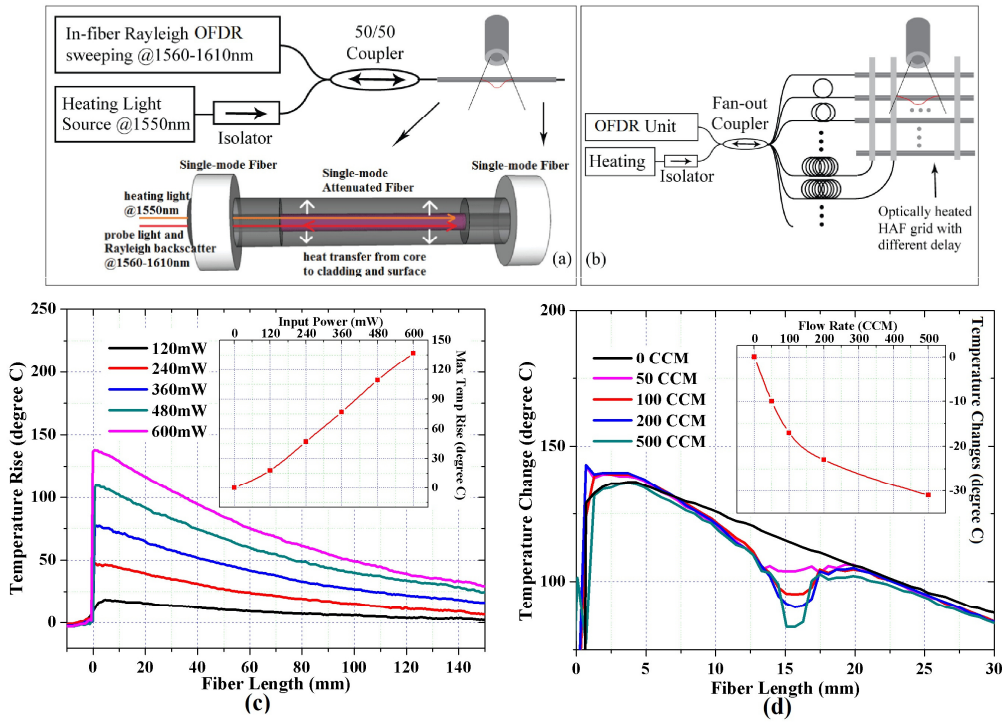

Fig. 5. (a) The schematic of flow sensing using OFDR and optical on-fiber heating; (b) Proposed setup for optically heated HWA grid; (c) The temperature profile and heating efficiency (Inset) for optical heating using 0.05dB/mm-loss HAF; (d) The flow sensor response and rate dependence (inset) using optical on-fiber heating.

Due to the nature of optical attenuation, optical-heated fiber sensing grid cannot be formed in serial. A parallel grid is proposed as shown in Fig. 5b to perform comprehensive flow measurement. The OFDR unit and heating light are coupled into parallel-multiplexed HAF HWAs, each having different optical delays to avoid spatial overlapping in Rayleigh measurements. Comparing with the electrical heating, the optical heating scheme fully exploited the advantages of fiber optic sensing, and are more suitable for flow sensing

#159670 - $15.00 USD Received 8 Dec 2011; revised 28 Feb 2012; accepted 28 Feb 2012; published 26 Mar 2012

applications in extreme environments such as strong EMI, conductivity and chemical corrosions. On the other hand, the optical attenuation and consequent non-uniform heating profile associated with optical heating scheme limited the dimensions and dynamic range of the measurements.

5. Conclusion

In conclusion, this paper presents a distributed fiber optical flow sensor using optical heated wire anemometry. The flow-induced heat loss profile on the fiber is spatially interrogated using OFDR Rayleigh scattering signals. By synthesizing the profile on every HWA section in the grid, comprehensive flow information including flow rate, position and direction was obtained with a single OFDR scan on a single fiber using one fiber feedthrough. Both electrical and optical on-fiber heated flow sensing were demonstrated to suit different sensing environments. Discrete gas flows and non-uniform flow fields can be identified with 1-cm resolution, while the displacement and tilting of individual flow can be tracked with sub-millimeter special resolution and <1° angular resolution. The high spatial resolution, simple installation, and wide adaptability to wide ranges of harsh environments make this sensing scheme useful for a wide range of industrial sensing applications.

Acknowledgments

This work was supported by the National Science Foundation (CMMI0644681 and CMMI-1054652) and the Department of Energy (DE-FE0003859).

#159670 - $15.00 USD Received 8 Dec 2011; revised 28 Feb 2012; accepted 28 Feb 2012; published 26 Mar 2012